Digital photogrammetry and kinematic GPS applied to the monitoring of Vulcano Island, Aeolian Arc, Italy

P. Baldi, S. Bonvalot, Pierre Briole, M. Marsella

Geophys. J. Int. (2000) **142,** 801–811

Digital photogrammetry and kinematic GPS applied to the monitoring of Vulcano Island, Aeolian Arc, Italy

P. Baldi,[1] S. Bonvalot,[2,3] P. Briole[3,4] and M. Marsella[5]

[1] *Università di Bologna, Dipartimento di Fisica,* 8 *viale B. Pichat,* 40126 *Bologna, Italy. E-mail: baldi@ibogfs.df.unibo.it*
[2] *IRD, Laboratoire de Géophysique,* 2 *avenue H. Varagnat,* 93143 *Bondy, France*
[3] *Institut de Physique du Globe de Paris,* 4 *place Jussieu,* 75005 *Paris, France*
[4] *UMR* 7580 *CNRS, Laboratoire de Sismologie,* 4 *place Jussieu,* 75252 *Paris, France*
[5] *Università di Roma 'La Sapienza', DITS,* 18 *via Eudossiana,* 00184 *Roma, Italy*

Accepted 2000 March 30. Received 1999 October 13; in original form 1998 November 30

SUMMARY

Digital photogrammetry and kinematic global positioning system (GPS) techniques are investigated and compared over a volcanic area as operational approaches to map the topography and monitor surface displacements. The use of terrestrial and airborne GPS to support the photogrammetric survey allowed for operational and processing time reduction without loss of accuracy. A digital elevation model (DEM) is obtained from the processing of the high-resolution digital imagery survey, which provides detailed information over a large area. The internal accuracy of the derived DEM has been verified by the comparison of two sets of data obtained from imagery acquired in different epochs; the observed root-mean-square error of residuals ranges from a few centimetres to 15 cm depending on the morphological features. Kinematic and pseudo-kinematic GPS surveys are performed to derive accurate 3-D coordinates at monumented benchmarks and accurate elevation profiles along footpaths. The average repeatability of the GPS measurements on benchmarks is 1 cm for measurement durations of 2–3 min. The standard deviation of interpolated vertical coordinates obtained at the crossings of kinematic GPS profiles is 4.3 cm. The high quality of these GPS coordinates justifies their use also for the validation of the photogrammetric DEM. A comparison of 6000 common points provides a standard deviation of residuals of 18 cm. The results show that the deformation pattern of a volcanic area can be rapidly and accurately monitored even in the absence of geodetic benchmarks. The integration of aerial photogrammetry with GPS kinematic surveys may be considered as an optimal approach for deriving high-resolution mapping products to be used in support of studies of volcanic dynamics.

Key words: deformation, satellite geodesy, topography, volcanic structure.

1 INTRODUCTION

The island of Vulcano (Southern Tyrrhenian Sea) is one of the active volcanoes of the Aeolian Arc. It is located along a very active fault system (Neri *et al.* 1991) and last experienced eruptive processes in 1888–1890. Its activity is characterized by eruptions separated by long intervals of low activity during which the central conduit is filled by solidified lava while fumarolic activity persists. Since 1987 some unrest has been observed, characterized by temperature increases, variation of the chemical composition of fumarole gases, the opening of new fractures and some (relatively low) seismic activity (Barberi *et al.* 1991). After the Patti earthquake (1978, $M = 5.5$), the northern part of the island was found to have subsided by about 15 mm relative to its southern part (Ferri *et al.* 1988); this deformation process was followed by a prolonged sinking of about 4 cm until 1981 (Frazzetta & La Volpe 1991). Subsequent surveys did not show any further significant deformation until 1990, when a small subsidence (20 mm) of the NW sector of the rim of La Fossa crater was observed (Obrizzo *et al.* 1994).

The activity of the volcano has been systematically monitored during the last 20 years by means of geodetic terrestrial measurements of distances and height differences, microgravimetric measurements and tilt stations. Large-scale aerial photogrammetry surveys have been performed in order to provide a more detailed description of the deformation patterns due to eruptive dynamics; from the analysis of the derived digital elevation model (DEM) it was also possible to study the side of the volcano affected by a landslide, which in 1988 produced a small tsunami in the harbour area (Achilli *et al.* 1998). The

advantage of photogrammetry is that it provides a full coverage of areas affected by surface modification and/or deformation phenomena. The classical geodetic approach, however, although usually characterized by higher accuracy, describes the deformation pattern on the basis of a limited number of points. Furthermore, recent developments in digital photogrammetry processing and the extensive use of aerial and terrestrial global positioning system (GPS) control points have resulted in operational and processing time reduction without loss of accuracy in the derived data sets.

With regard to terrestrial surveys, the advent of GPS has greatly improved the methodology for ground deformation monitoring, allowing one to collect higher-accuracy and higher-density data with simplified and faster operations in the field. Today this technique is often used as an alternative to ground-based topographical methods such as levelling or trilateration (Camitz *et al.* 1995; Pingue *et al.* 1998). More recently, the appearance of a new generation of receivers has allowed the surveying of geodetic networks in very short periods of time (a few minutes occupation of points in quick-static mode and a few seconds in pseudo-kinematic mode instead of one to several hours in static mode), keeping the accuracy at about 1 cm in the horizontal and 2 cm in the vertical. With respect to the previous way of using GPS, this new method allows a further increase in the number of surveyed points and at the same time decreases the duration of the geodetic campaigns. Whilst a GPS receiver is operated at a fixed reference station, the survey is performed with a roving GPS receiver that is left operating during the whole measurement session on the benchmarks and during the move between two benchmarks. In this manner, in addition to the periods corresponding to measurements at a benchmark, the entire trajectory of the antenna is also recorded. With a typical sampling rate of 1–3 s, this represents thousands of coordinates recorded along a path of a few kilometres that can be surveyed in a few hours.

After the evaluation of the accuracy of our kinematic GPS measurements obtained with various field procedures (driving or walking mode), the GPS profiles are used for the assessment of the accuracy of the digital-photogrammetry-deduced DEM. On the basis of these results it was possible to establish the threshold level of deformation detectable on Vulcano by comparing DEMs derived from different images. In addition, the GPS profiles are also examined in order to determine the areas were kinematic positioning could be successfully used for future surveys at Vulcano.

2 GPS AND DIGITAL PHOTOGRAMMETRY PROJECTS OVER VULCANO ISLAND

Photogrammetric surveys were performed over Vulcano Island in 1971, 1983 and 1993 in order to acquire images at a scale of 1:10 000 and 1:5000. In order to process digitized images from the 1983 and 1993 projects, a digital photogrammetric station, Helava (DPW710) (Miller *et al.* 1995), was used. Using the internal automatic correlation module, two 5 m grid DEMs were generated from the 1983 and 1993 data. The comparison between the two models resulted in a mean standard deviation of the differences in the height coordinates of about 0.5 m (Achilli *et al.* 1998) and allowed the estimation of the terrain volume involved in the major landslide in 1988 that affected the northeastern side of the volcanic cone, producing a small tsunami in the neighbouring harbour (Tinti *et al.* 1999). These results encouraged further digital photogrammetry experiments for extracting highly accurate mapping products useful for controlling volcanic areas. The integration of GPS and photogrammetry provided a more powerful monitoring tool because of the reduction in time and cost of the field operations.

Thus, in September 1996 the use of GPS for collecting both terrestrial and aerial control points was investigated in conjunction with an aerial photogrammetry survey performed over the island (Achilli *et al.* 1997). The images were taken at two different flight heights in order to obtain 1:5000 and 1:10 000 photo scales. Fig. 1 shows the photographic coverage for the 1:5000 flight.

An accurate GPS control network was established in the survey area by placing 22 specially designed aerial targets (Fig. 1)—also called ground control points (GCP)—on the ground. GPS receivers were continuously operating on three master GCP while the rest of the targets were measured during sessions of about 30 min. The GPS network adjustment indicated a standard deviation of a few millimetres in the horizontal components and 1–2 cm in the vertical component (Achilli *et al.* 1998).

The aircraft was equipped with a WILD RC20 camera communicating with two GPS receivers connected to the same antenna mounted on the fuselage. The three reference GCP on the island and one at the airport of Reggio Calabria, 70 km distant from the investigated area, were used for determining high-accuracy aircraft trajectory with an 'On-The-Fly' kinematic GPS procedure.

2.1 Aerial GPS data for controlling photogrammetry

A GPS photogrammetry survey implies the use of GPS receivers both to establish the ground reference network and to determine aerial 3-D coordinates of the camera position at

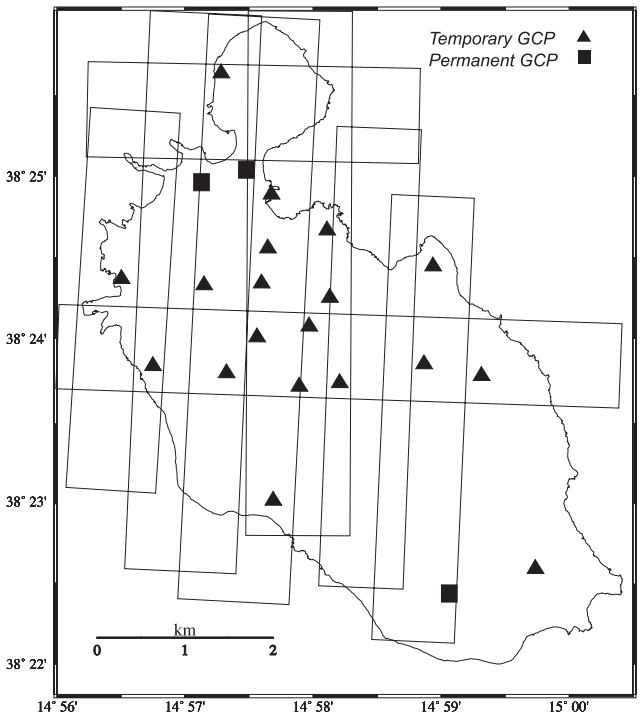

Figure 1. Location of ground control points and coverage of the photos for a 1:5000 scale flight.

the instant of exposure. Knowledge of the camera coordinates allows the introduction of additional equations into the aerial triangulation (AT) least-squares adjustment procedure and, as a consequence, the number of required ground control points can be significantly reduced (Colomina 1993). Therefore, GPS photogrammetry is highly simplified in remote areas such as volcanoes where a homogenous ground targets network is difficult to install.

The GPS data collected from the aircraft and at the three reference GCP with a sampling rate of 1 s were processed using different software developed for handling kinematic data and including On-The-Fly ambiguity solution algorithms. The results obtained provided trajectories of the aircraft with differences at a centimetre level (Baldi *et al.* 1998). After interpolating at the instant of photo exposure and reducing the GPS antenna position at the camera centre, the GPS aerial control was derived in the form of three parameters (3-D WGS84 coordinates) of the camera orientation. These angular parameters can be used as additional constraints to enforce the AT adjustment and thus again reduce the number of required GCP.

In order to assess the accuracy achievable on GPS-aided aerial triangulation adjustments, an analysis has been performed using data selected over a test area covering the central part of the cone. True terrain coordinates (ENU) of the 12 GCP were derived from the GPS static solution of the control network. The observed image coordinates were processed with the program GAPP (GPS Assisted Phototriangulation Package) for bundle block adjustment. The solution was obtained for different cases in order to derive accuracy parameters while using a decreasing number of control points. The eliminated points were introduced into the bundle adjustment as checkpoints and their estimated coordinates were directly compared with their true values. The rms values of the differences between adjusted and true coordinates represent the absolute accuracy of the adjusted block (Table 1). The comparison between the 7GCP and the 4GCP cases, in which seven and four GCP, respectively, were adopted, demonstrates that the use of three more GCP does not lead to any significant improvement in the vertical component of the adjusted coordinates. This can be explained by the optimization already obtained by the introduction of high-accuracy GPS coordinates for the position of the camera centres as aerial control points. Furthermore, the four control points selected for the 4GCP are located at the bottom of the volcano and thus can be easily established and measured. The 2GCP case may represent the practical case of minimal control since only the camera position coordinates are available from GPS and the attitude parameters are to be estimated. Ground control is necessary not only to stabilize the block but also for solving the datum problem in order to transform the coordinates into a state coordinate system. The resulting accuracy for the 2GCP case is still equivalent to cases in which, in the absence of GPS camera station positions, a very dense ground control model is needed.

Table 1. Standard deviations of differences between static GPS coordinates of checkpoints and those resulting from aerial triangulation adjustment performed using different control point configurations.

GPS_AT	Standard. deviation		
	East (cm)	North (cm)	Up (cm)
7 GCP	2	3	10
4 GCP	5	6	8
2 GCP	12	9	18

2.2 Digital photogrammetry processing

In digital photogrammetry, the same principles and methods as for classical photogrammetry are applied. The products are point coordinates, graphic and/or numerical maps and rectified images. The processing of the images is carried out using matching procedures that are based on well-defined shape comparison techniques or on the levels of grey in the homologous zones of the images (Kraus 1994; Heipke 1995). The main parameters that control the accuracy of the restitution are the scale and resolution of the image or photo; if we assume a 1000 dpi resolution, which results in a pixel size of 25 μm, we obtain a corresponding dimension of the pixel on the ground of 6 and 25 cm for image scales of 1:2500 and 1:10 000, respectively. The capability of the correlation algorithms to work at subpixel level, the quality of the image, the presence of shadows and the morphology of the surface also determine the final accuracy of the digital products.

For the 1996 photogrammetric survey, a block formed by five strips including 23 photos was analysed using the Helava system (Miller *et al.* 1995). The images were digitized using a scanner coupled with a Helava DPW710 at a resolution of 1000 dpi. At the 1:5000 scale the corresponding ground pixel resolution is about 12.5 cm. Using the image automatic correlation module, a 1 m grid DEM of the central part of the volcano was generated, allowing us to define at high spatial resolution the shape of the caldera structure (Fig. 2).

In order to evaluate the internal accuracy of the derived elevations, two digital models obtained by processing stereo pairs acquired in 1993 and 1996 at a 1:5000 scale were compared. The two photogrammetric models were processed assuming a common absolute orientation and adopting the same image automatic correlation module for DEM extraction. The selected region for DEM comparison included different morphological features, varying from highly sloping areas to smooth terrain and including also the area involved in the 1988 landslide (Fig. 3).

Fig. 4 shows the difference between the two DEMs. The rms of residuals is a few centimetres in the smooth summit area and increases to 5–15 cm for the more corrugated northern slopes of the cone. Large differences (20–40 cm) are evident at the border of the 1988 landslide and in some limited areas. Such differences can be interpreted as local topography changes between 1993 and 1996.

3 KINEMATIC GPS DATA

3.1 Vulcano kinematic GPS survey

A kinematic GPS survey was carried out on Vulcano Island from 4 to 8 June 1997 (Julian days 155–159). Measurements were performed in a differential mode with 12-channel dual-frequency receivers with full-wavelength data (P-code) using Z-tracking technology, i.e. the Ashtech Z-XII Surveyor model. Two reference GPS base stations were operated at the volcanological observatory CO (Centro Operativo) during the whole

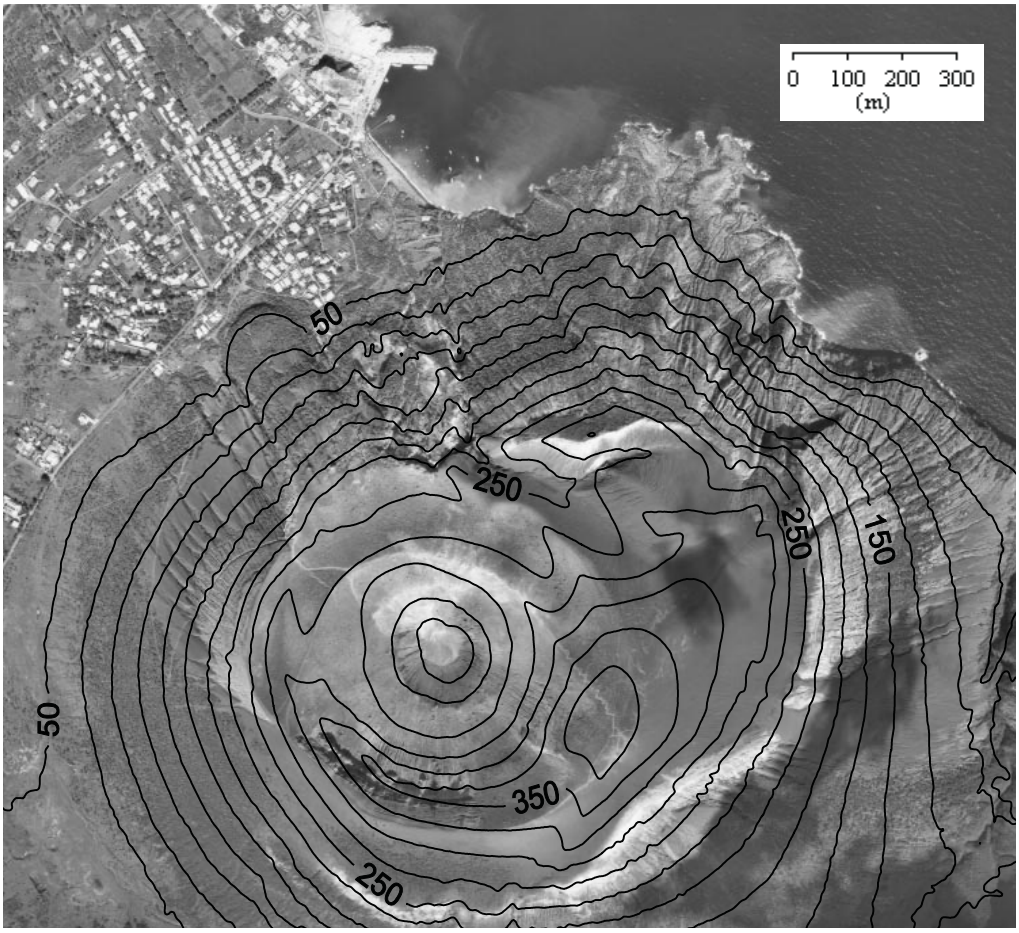

Figure 2. Photogram of the cone of Vulcano crater, the town and the harbour (Porto Levante) with contour lines (metres) extracted from the 1996 DEM.

survey. The baseline length for differential observations between mobile receivers and reference stations is less than 4 km. Ashtech Light Marine LIII and geodetic antennae were used for mobile and reference receivers, respectively. Fig. 5 shows the distribution of the differential GPS profiles performed during the survey.

The data acquisition was performed in order to evaluate several kinematic field procedures expected to give accurate elevation measurements in real time or post-processing. The On-The-Fly initialization used to resolve integer ambiguity on carrier phase measurements for each epoch requires continuous observations, without gaps in the data acquisition. Gaps are

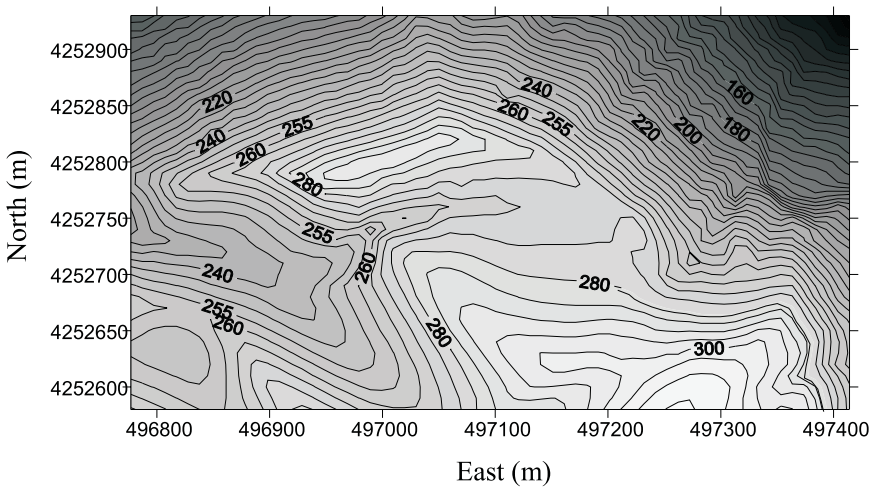

Figure 3. Contour lines (5 m) of the sample area used for the comparison of the 1993 and 1996 photogrammetry-derived DEM (UTM reference system).

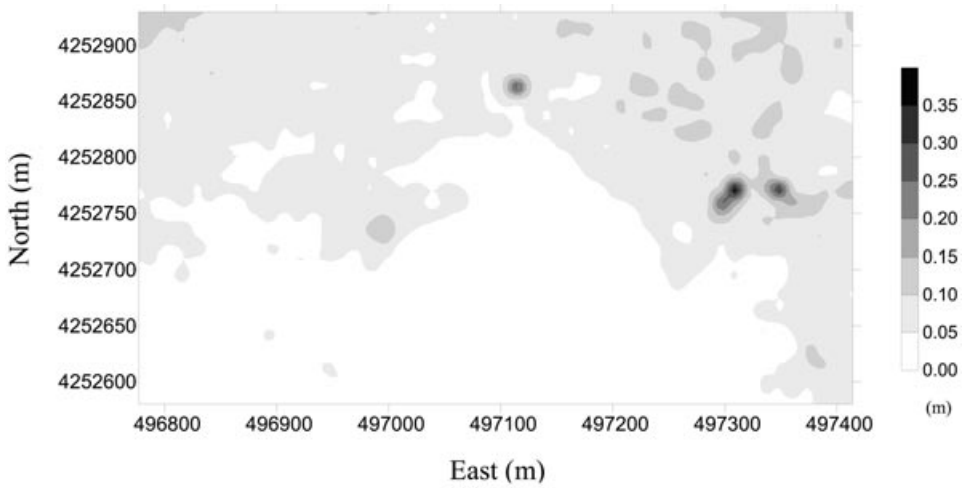

Figure 4. Areal distribution of rms error of differences (DEM93 – DEM96); the darker areas on the right of the figure are located along the border of the zone involved in the major 1988 landslide.

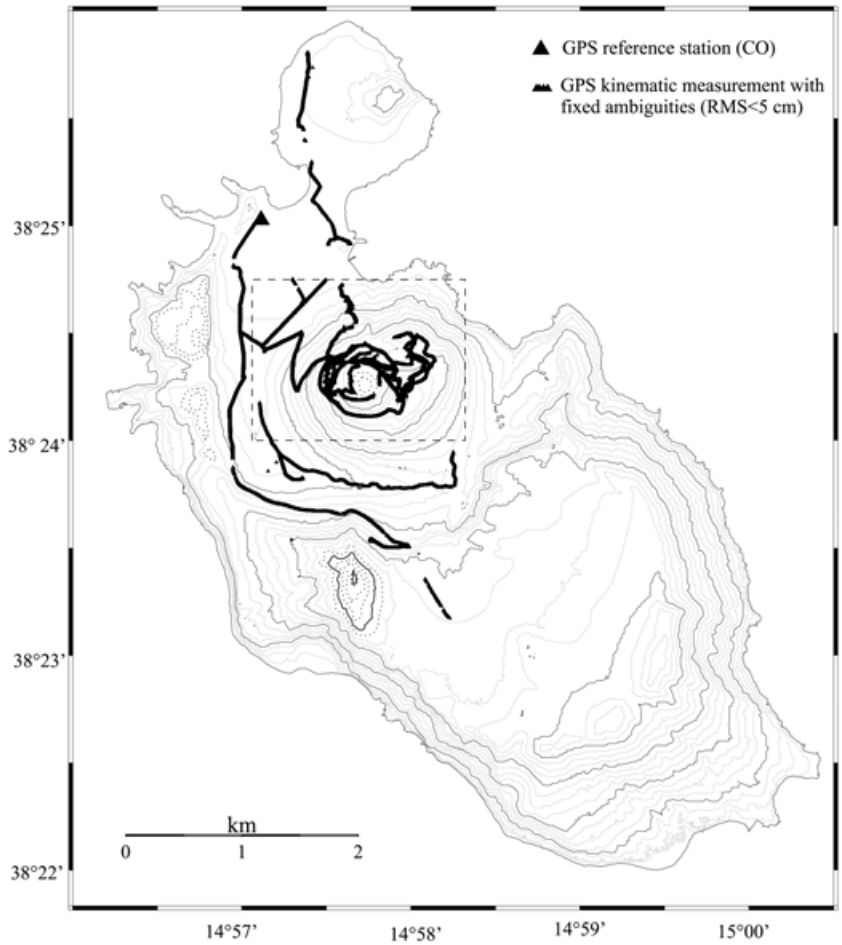

Figure 5. Kinematic GPS survey at Vulcano island (June 1997). Location of differential GPS profiles performed between June 4 and 8 1997 with Ashtech Z12 Surveyor receivers. Measurements were performed in driving mode (antenna mounted on car) along roads and tracks outside the active area and in walking mode (antenna mounted on telescopic pole held by bipod or on backpack) over La Fossa crater area. Only measurements with fixed ambiguity solutions (rms scatter <5 cm) are considered. Two reference GPS base stations were set up at the volcanological observatory CO (Centro Operativo) during the kinematic survey. Dashed box outlines the crater area (see Fig. 6a). Topographic contour intervals of 100 m and 20 m are represented by solid and dotted lines, respectively.

induced by bad reception (a mask over the antenna), leading to a loss of tracked satellites and consequently to a decrease in the accuracy of the kinematic positioning. Even though the data post-processing procedures reduce the amount of unusable data by means of forward and backward processing, special care was taken during the field measurements to ensure the continuity of the data recording.

With this aim, two procedures have been tested during the Vulcano kinematic survey for gathering continuous recordings according to the field conditions. Around the active cone, we acquired kinematic profiles along the main road and tracks in driving mode (Fig. 5). The antenna was mounted on the top of a car and the measurements were continuously acquired during vehicle motion. The acquisition rate was set to 1 s for a car speed of about 20–30 km hr^{-1}, leading to a typical distance of 5–10 m between adjacent samples. On the crater area, data were acquired in a walking mode, with the antenna mounted on the operator's backpack, with an acquisition rate of 2 s ($\sim$2 m between adjacent data collections). In both procedures, the antenna could be easily moved from the car or the backpack

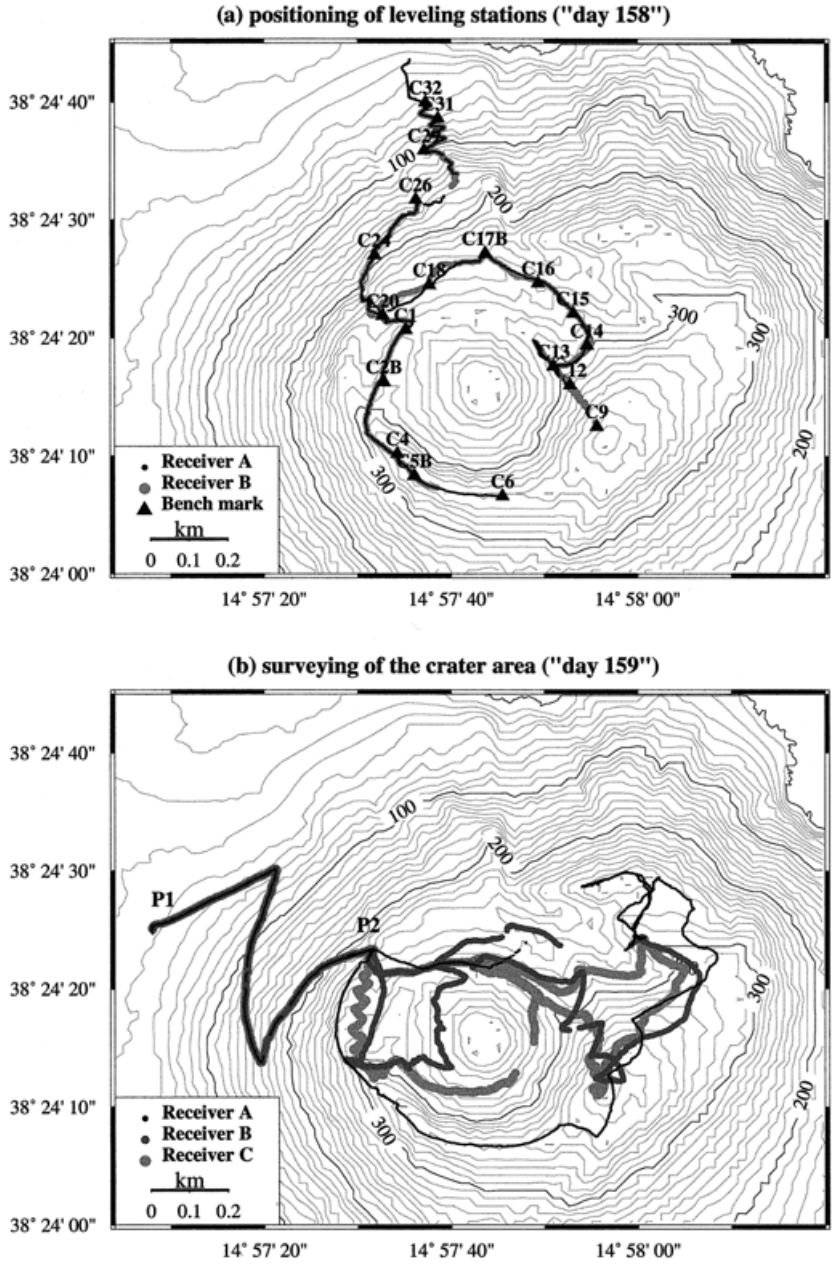

Figure 6. Detailed view of GPS kinematic profiles in the active area. (a) Kinematic positioning of levelling stations (day 158) performed in walking mode with antenna mounted on telescopic pole held by bipod. The observations were performed on benchmarks with two receivers in a round-trip survey (acquisition rate 2 s). The durations of sessions ranged roughly between 3 and 5 min. (b) Surveying of the crater area (day 159) performed with three receivers in walking mode with antenna mounted on backpack. The measurements were recorded continuously with a 2 s sampling rate whilst walking around and inside La Fossa crater for DEM control. P1 and P2 are the start- and endpoints of the access path to the La Fossa crater followed by receivers A, B and C. Topographic contour intervals of 100 m and 10 m are represented by solid and dotted lines, respectively.

and mounted on a telescopic pole or on a geodetic tripod for the measurement of monumented benchmarks. The only cause of interruption in data collection during the Vulcano survey came from masks due to the presence of trees or buildings along some road sections. The point locations along the kinematic profiles reported in Fig. 5 only show measurements for which fixed ambiguity solutions were resolved during post-processing of the data. It can be seen that profiles in the crater area do not exhibit discontinuities. This property is a consequence of the sparseness of vegetation and confirms that the kinematic GPS method is fully appropriate to the surveying of the La Fossa di Vulcano crater area.

The observations were performed with at least two or three receivers to allow a comparison of the results and thus an evaluation of the internal accuracy and the repeatability of the kinematic measurements. Results from intercomparison and crossover error analysis of the data as well as the evaluation of the internal accuracy of the GPS survey are discussed in the next sections. The observations were carried out on 7 June 1997, hereafter called 'Day 158', and 8 June 1997, hereafter 'Day 159'.

In order to check the accuracy of the height determination by kinematic GPS positioning, day 158 was mostly dedicated to the positioning of levelling stations. Measurements on 19 stations of the levelling network, which is frequently measured for deformation studies, were performed (Obrizzo *et al*. 1994). These benchmarks are distributed along a profile extending from the base to the summit of the cone and around the La Fossa di Vulcano crater (Fig. 6a). Most of these stations were successively measured with two receivers (A and B) and some of them were occupied twice with the same receiver in the direct and reverse ways. For each benchmark, the data were acquired in a continuous mode with a sampling rate of 2 s during each time interval, which typically ranged from 2–5 min. The antennae were mounted on a telescopic pole during fixed positioning on levelling benchmarks and on the operator's backpack between two stations.

Day 159 was dedicated to the surveying of the active area. A detailed survey of the crater was made with three receivers (A, B and C) used in walking mode with antennae mounted on the operators' backpacks (Fig. 6b). The data were continuously

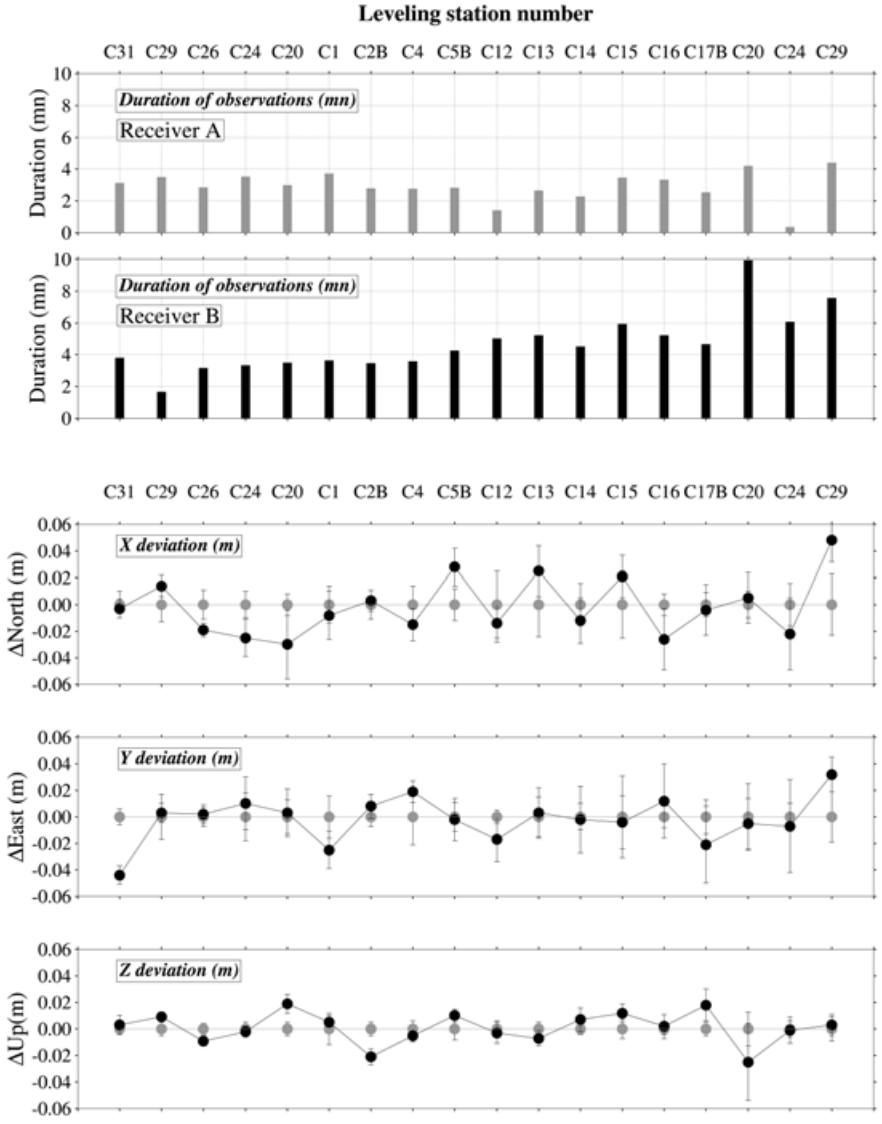

Figure 7. Internal accuracy of GPS positioning on levelling stations for day 158. Deviations in horizontal and vertical mean coordinates for receiver B are plotted with respect to receiver A. The deviation in altitude is ± 3 cm.

recorded with a 2 s sampling rate around and inside La Fossa crater for the DEM validation. In order to control the accuracy of the measurements, data were acquired with the three receivers at many common observation sites such as on the access path to the crater area (for altitudes from 40 to 220 m) and at track crossings.

The data from both days have been used for the DEM accuracy assessment.

3.2 Data processing

The processing of the data was performed by means of the Ashtech precise differential GPS navigation and surveying software PNAV6 v2.5 (Ashtech 1995). Only solutions with fixed ambiguities were kept in this study. In practice, this corresponds to observations with a minimum of 5–6 common satellites, as mentioned by Deplus & Briole (1997). The present software version does not allow one to include observed troposphere parameters; we used a standard model ($Td = 20$ °C, $Tw = 14$ °C, $Po = 1013$ hPa), but considering the amplitude of the topographic variations within the surveyed area (less than 400 m), its small extension (baseline lengths less than 4 km) and the good weather conditions during the survey, this approximation could not introduce errors greater than 5 mm in the computed relative coordinates.

3.3 Internal accuracy of GPS measurements

3.3.1 Comparison of measurements on levelling stations (day 158)

Fig. 7 shows a comparison of the two kinematic routes of day 158 on levelling stations where repeated measurements with two receivers have been performed. The duration of individual data records ranges from 30 s to 10 min, with a mean value of about 2–3 min. The differences between the computed coordinates for receiver B and receiver A are plotted for each session, with the receiver A used as a reference. These differences are in the range of ± 5 cm and ± 3 cm for the horizontal and vertical coordinates, respectively. The lower accuracy in the horizontal coordinates is due to the fact that the antenna is not fixed on a tripod but handled by the operator, a bubble level being used to maintain verticality. This result confirms that a positioning at a few centimetres accuracy can easily be obtained over this area with the kinematic method, with low logistic constraints, for sessions of data collection of the order of a few minutes (typically 3–5 min). Considering the accuracy and speed of use, such a procedure appears to be efficient complement to the classical methods of geodetic monitoring at Vulcano. Table 2 contains the mean values of ITRF94 (IERS Terrestrial Reference Frame 1994, Boucher *et al.* 1996) horizontal and vertical coordinates of the levelling stations computed from the GPS data sets A and B. The rms scatter is about 1 cm in both horizontal and vertical determinations. Point VU04 belongs to a large GPS network (the Tyrgeonet network) and its coordinates (Anzidei *et al.* 1995) were used as a reference for the whole survey.

3.3.2 Crossover error analysis of the kinematic survey (days 158 and 159)

In order to check the internal accuracy of the kinematic GPS data set acquired in the active area, a crossover error (COE) analysis was performed on tracks surveyed with various receivers for days 158 and 159. The COE analysis is based on the computation of the discrepancies in height determinations calculated at the intersections of independent track lines. The height value along a given track at a crossover point is obtained

Table 2. ITRF94 coordinates of the levelling points observed during the 1997 GPS survey on Vulcano Island (Fig. 6a) and standard deviation of the points measured more than once. The number of occupations is listed in the last column. The rms scatter is about 1 cm in both the horizontal and the vertical directions.

Point	Latitude (ITRF94)	rms scatter (m)	Longitude (ITRF94)	rms scatter (m)	Altitude (ITRF94)	rms scatter (m)	Number of observations
VU04	38 25 1.69616		14 57 6.92156		51.107		
C4	38 24 10.16525	0.010	14 57 34.25717	0.007	387.813	0.002	2
C5B	38 24 8.27226	0.001	14 57 36.06545	0.014	395.001	0.005	2
C6	38 24 6.56953		14 57 45.51152		398.820		1
C9	38 24 12.45935		14 57 55.58897		429.780		1
C12	38 24 15.97230	0.009	14 57 52.73377	0.007	371.920	0.002	2
C13	38 24 17.56271	0.001	14 57 50.94338	0.013	350.022	0.004	2
C14	38 24 19.33592	0.001	14 57 54.54691	0.006	347.008	0.003	2
C15	38 24 22.05328	0.002	14 57 53.07116	0.010	326.892	0.006	2
C16	38 24 24.60827	0.006	14 57 49.31345	0.013	304.636	0.001	2
C17B	38 24 27.14220	0.011	14 57 43.65518	0.002	293.995	0.009	2
C18	38 24 24.44666		14 57 37.66921		295.445		1
C19	38 24 24.44717		14 57 37.66925		295.412		1
C20	38 24 21.83962	0.004	14 57 32.69999	0.010	301.471	0.011	4
C24	38 24 27.01199	0.004	14 57 31.81316	0.012	247.786	0.015	4
C26	38 24 31.69876	0.007	14 57 36.22637	0.010	204.008	0.005	3
C29	38 24 35.87364	0.009	14 57 37.12158	0.018	138.187	0.003	4
C31	38 24 38.56100	0.016	14 57 38.62130	0.006	92.724	0.002	3
C32	38 24 39.93937		14 57 37.28736		77.896		1

by interpolation of the data along the particular track. The analysis assumes that no large errors affect the determination of horizontal coordinates that are used to compute intersections between track lines. For coordinates obtained with an ambiguity fixed solution, it was shown in the previous section that the horizontal accuracy is of the order of ± 5 cm. A similar accuracy was found by Deplus & Briole (1997) for their 3-D determination of single points sampled along kinematic GPS profiles. Assuming this accuracy, the analysis of the residuals between height determinations can be discussed in terms of a normal distribution, leading to an estimation of the mean value and the standard deviation of the distribution. The algorithm used in this study for the COE was proposed by Hsu (1995).

Although special care was taken in attempting to attain continuous data acquisition with a regular spacing (constant operator speed), a few stops were made by operators during the survey. In order to optimize the data comparison, the redundant data that were obtained at these pseudo-fixed

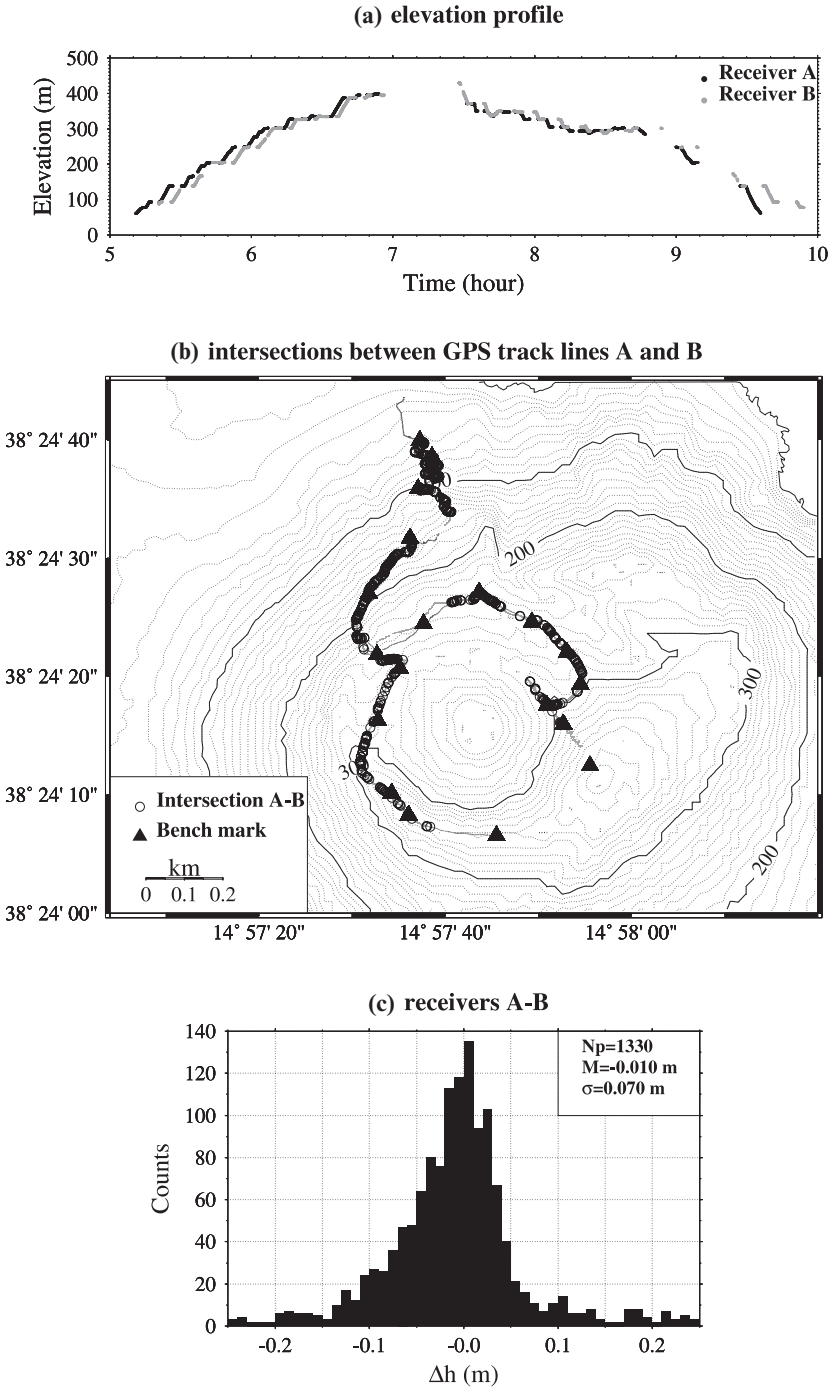

Figure 8. Results of the COE analysis of GPS measurements for day 158. (a) Elevation profiles acquired with both receivers in mobile mode. (b) Map of the locations of the computed intersections between GPS profiles used for the comparison. (c) Histogram of the distribution of the difference in heights obtained with receivers A and B at profile intersections. The parameters Np, M and σ define the number of intersections, the mean value and the standard deviation of each distribution.

positions and where changes in the height of antennae were partly due to irregular vertical movements of the operator or operator's backpack were removed. Such data, however, represent less than 2 per cent of the data collection for each receiver.

The results of the COE analysis for day 158 are given in Fig. 8. Only data acquired in mobile mode along the profile have been retained for this analysis (Fig. 8a). A total of 1330 intersection points were computed from the data set. The locations of these intersection points between GPS track lines are shown in Fig. 8(b). The differences between elevations at the intersection points for receivers A and B are centred on a mean value of about 1 cm with a standard deviation of 7 cm (Fig. 8c).

Fig. 9 shows the results of the COE analysis of the whole GPS data set for day 159. The histogram displays the distribution of the differences in the height determinations obtained with receivers A, B and C at profile intersections. The observed COE distribution exhibits the shape of a normal-frequency distribution with central values close to zero. The mean value of the COE is centred on 1 mm, with a standard deviation of 4.3 cm for 4975 intersection points. Detailed results from comparisons of receiver pairs (Table 3) reveal that standard deviations are lower for the same track (2–4 cm) than for two different tracks (5–7 cm). These results are consistent with the expected accuracy for such kinematic surveys in walking mode with antennae mounted on operators' backpacks as specified by Ashtech (1995). Clearly, such GPS data are sufficiently accurate to control and validate high-resolution DEM derived from digital photogrammetry.

4 COMPARISON OF DEM AND KINEMATIC GPS DATA

Using the directly determined height (by kinematic GPS) it was possible to assess the quality of the photogrammetric DEM. The automatic photogrammetric procedure described above was adopted to generate a DEM for a 1 m × 1 m grid. The control network was surveyed by using GPS receivers and

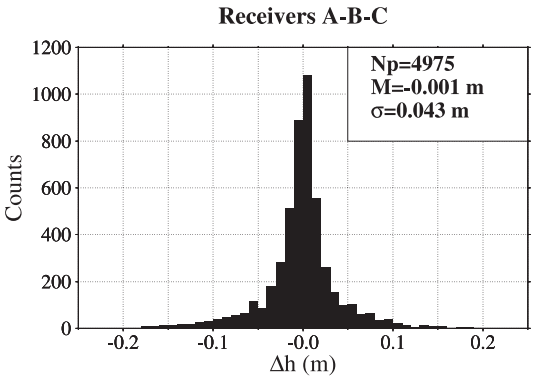

Figure 9. Results of the COE analysis of GPS measurements for day 159 (Fig. 6b). The histogram shows the distribution of the differences in the height determinations obtained with receivers A, B and C at profile intersections. Np, M and σ are, respectively, the number of intersections, the mean value and the standard deviation of the distribution. The distribution of the COE has a normal-frequency pattern with a mean value close to zero. Detailed results for each pair of receivers are given in Table 3.

Table 3. Results of the COE analysis of kinematic GPS profiles performed in the La Fossa crater area with receivers A, B and C (Fig. 6b). The differences in the height determinations obtained with each pair of receivers at profile intersections revealed a normal-frequency distribution pattern. *Np*, *M* and σ are, respectively, the number of intersections, the mean value and the standard deviation of the distribution computed for each pair of receivers.

Receiver pair	*Np*	*M* (m)	σ (m)
A–A	298	−0.012	0.038
B–B	930	−0.002	0.035
C–C	1792	0.002	0.022
A–B	661	0.007	0.049
A–C	477	−0.007	0.056
B–C	817	−0.008	0.068

computed in the ITRF94 reference system by establishing three fixed reference stations tied to the international reference network. Two of these points were used as base stations for the kinematic GPS surveys, allowing us to refer the two sets of data to the same reference system. This fact allows us to compare directly the elevations derived from the two methods. From the GPS kinematic data set, we extracted the points located within a 20 cm radius of a grid node in order to minimize the interpolation effects. Therefore, the comparison was performed over about 6000 corresponding points, mainly distributed around the top of the active cone. Two different interpolation methods (kriging and low-order polynomials) were then used for extracting from the DEM the heights corresponding to the GPS points. The two approaches provided similar results.

In a preliminary analysis the comparison of the GPS kinematic- and DEM-derived heights evidenced a bias that can mainly be attributed to the offset between the GPS phase centre of the rover antenna and the ground. After the removal of the observed offset, the data show a Gaussian distribution pattern where almost all the residuals are within ± 50 cm and the resulting standard deviation is 18 cm (Fig. 10). This result, obtained using independently derived data, confirms the high accuracy and reliability of the digital photogrammetric technique for producing a DEM of areas involved in deformation processes.

5 CONCLUSIONS

A high-resolution 1 m × 1 m grid DEM of the crater area of Vulcano island (Italy) has been derived using digitized images at a scale of 1:5000 acquired during a GPS photogrammetry survey. An external comparison with about 6000 elevation values obtained from a kinematic GPS survey shows good agreement between the two sets of vertical coordinates, with a standard deviation of differences of 18 cm. The comparison with a previous photogrammetry DEM shows that the average difference ranges from a few centimetres in flat areas to 5–15 cm in corrugated areas. Large differences (20–40 cm) are evident at the border of the 1988 landslide and in some limited areas. Such differences can be interpreted as local topography changes between 1993 and 1996. Geodetic points should be set up in the moving area evidenced in our data in order to confirm this result and provide further monitoring of the deformation of this area.

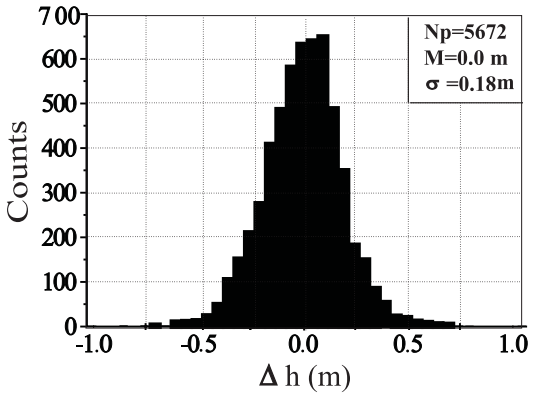

Figure 10. Distribution of the differences in the height coordinates derived from the comparison between kinematic GPS measurements and GPS photogrammetry-derived DEM in the Vulcano crater area (Fig. 2). The 1 m pixel size DEM has been generated from a photogrammetric block at 1:5000 scale (Fig. 1). A selection of about 6000 GPS height values obtained from kinematic coordinates located within 20 cm of DEM grid nodes was used for the DEM accuracy assessment. The rms standard deviation is 18 cm.

During the kinematic GPS survey, several field procedures were tested over the active area in order to estimate the accuracy of this new technique for the fast positioning of geodetic stations or for the production of precise DEMs. The internal accuracy of the kinematic data has been evaluated by means of a Crossover error analysis between various GPS tracks. Accurate elevation measurements can easily be obtained within a range of ± 3 cm for a data collection of about 3–5 min on a fixed point. This level of accuracy achieved in a short session time enhances the relevance of the kinematic technique for volcano monitoring. This method appears to be complementary to static GPS surveys and classical geodetic methods. It allows one to measure a large number of points. The crossover error analysis of the kinematic GPS profiles in the crater area indicates vertical scatter of between 3 and 10 cm, with a mean value of 4.3 cm. Furthermore, such elevation data sets, which can easily be collected during field surveys, are particularly suitable as a field check of high-resolution digital models such as those derived from photogrammetry. These results confirm the possibility of monitoring at high spatial resolution and within an error range of few centimetres the deformation processes of volcanic areas whether or not they are equipped with geodetic benchmarks on the ground.

The integration of aerial photogrammetry with GPS kinematic surveys may be considered as an optimal approach for the digital mapping of such areas as the study of the volcano dynamics.

ACKNOWLEDGMENTS

We thank Jérôme Ammann (IPG Paris), Franco Obrizzo (Osservatorio Vesuviano, Napoli), Jean Vandemeulebrouck (Université de Chambéry) and Alessandro Bonforte (IIV Catania) for their assistance during the GPS kinematic survey, Christine Deplus for helpful discussion about the COE analysis technique and Marco Anzidei (ING Roma) for encouraging this work. Some figures presented in the paper have been drawn with the GMT 3.0 software (Wessel & Smith 1995). This work was supported by CNR, Gruppo Nazionale di Vulcanologia, by EC contract AVMS (ENV4-CT96–0250), by the Département des Observatoires Volcanologiques de l'IPGP (IPG contribution no. 1673) and by the Département Milieux et Environnement de l'IRD.

REFERENCES

Achilli, V., Anzidei, M., Baldi, P., Marsella, M., Mora, P., Targa, G., Vettore, A. & Vittuari, L., 1997. GPS and digital photogrammetry: an integrated approach for monitoring ground deformations on a volcanic area, in *Proc. ISPRS WG VI/3 'International Cooperation and Technology Transfer' Mtng, Padova,* pp. 1–5, eds Mussio, L., Crippa, B. & Vettore, A., Politecnico di Milano, Italy.

Achilli, V., Baldi, P., Baratin, L., Bonini, C., Ercolani, E., Gandolfi, S., Anzidei, M. & Riguzzi, F., 1998. Digital photogrammetric survey on the island of Vulcano, *Acta Vulc.,* **10,** 1–5.

Anzidei, M., Baldi, P., Casula, G., Riguzzi, F. & Surace, L., 1995. La rete Tyrgeonet, *Boll. Geod. Sci. Affini,* **LIV** (2), 1–19.

Ashtech Process User's Guide, 1995. *Prism Software,* Ashtech Inc, Sunnivale, CA.

Baldi, P., Marsella, M. & Vittuari, L., 1998. Airborne GPS performance during a photogrammetric project, in *IAG Scientific Assembly, Rio de Janeiro, Proceedings Series*, Vol. 118, pp. 343–348, Springer Verlag, Berlin.

Barberi, F., Neri, G., Valenza, M. & Villari, L., 1991. 1987–1990 unrest at Vulcano, *Acta Vulc.,* **1,** 95–106.

Boucher, C., Altamimi, Z., Feissel, M. & Sillard, P., 1996. Results and analysis of the ITRF94, *IERS Technical Note*, 20, Observatoire de Paris, Paris.

Camitz, J., Sigmundsson, F., Foulger, G., Jahn, C.H., Volksen, C. & Einarsson, P., 1995. Plate boundary deformation and continuing deflation of the Askja volcano, North Iceland, determined with GPS, 1987–1993, *Bull. Volc.,* **57,** 136–145.

Colomina, I., 1993. A note on the analytic of aerial triangulation with GPS aerial control, *Photogrammetric Eng. Rem. Sens.,* **59,** 1619–1624.

Deplus, C. & Briole, P., 1997. Mesure de profils par GPS cinématique, Résultats d'un test effectué en Crète en Octobre 1996, *Internal Rept,* IPG, Paris.

Ferri, M., Grimaldi, M. & Luongo, G., 1988. Vertical ground deformation on Vulcano, Aeolian Island, Southern Italy: observations and interpretations 1976–1986, *J. Volc. Geotherm. Res.,* **35,** 141–150.

Frazzetta, G. & La Volpe, L., 1991. Volcanic history and maximum expected eruption at 'La Fossa Vulcano' (Aeolian Islands, Italy), *Acta Vulc.,* **1,** 107–115.

Heipke, C., 1995. State-of-the-art of digital photogrammetric workstations for topographic applications, *Photogrammetric Eng. Rem. Sens.,* **61,** 49–56.

Hsu, S.K., 1995. XCROSS: a cross-over technique to adjust track data, *Computers Geosci.,* **21,** 259–171.

Kraus, K., 1994. La fotogrammetria digitale, *Fotogrammetria,* **1,** 447–498.

Miller, S., Helava, U.V. & Devenecia, K., 1995. Softcopy photogrammetric workstations, *Photogrammetric Eng. Rem. Sens.,* **61**, 49–56.

Neri, G., Montalto, A., Patane', D. & Privitera, E., 1991. Earthquake space-time magnitude pattern at Aeolian Islands (Southern Italy) and implications for the volcanic surveillance of Vulcano, *Acta Vulc.,* **1,** 163–169.

Obrizzo, F., Del Gaudio, G. & Ricco, C., 1994. Vertical ground movements, in *Data Related to Eruptive Activity, Unrest Phenomena and Other Observations on the Italian Active Volcanoes,* ed. Villari, L., *Acta Vulc.,* **6,** 61–63.

Pingue, F., De Troise, C., Luca, G., Grassi, V. & Scarpa, R., 1998. Geodetic monitoring of Mt. Vesuvius Volcano, Italy, based on EDM and GPS surveys, *J. Vol. Geotherm. Res.,* **82,** 151–160.

Tinti, S., Bortolucci, E. & Armigliato, A., 1999. Numerical simulation of the landslide-induced tsunami of 1988 in Vulcano island, Italy, *Bull. Volc.,* **61,** 121–137.

Wessel, P. & Smith, W.H.F., 1995. New version of the Generic Mapping Tools released, *EOS, Trans. Am. geophys. Un.,* **76,** 329.